JOURNAL OF MATERIALS SCIENCE 23 (1988) 2546–2552

Highly oriented single-phase blend films of high- and low-density polyethylene

DECAI C. YANG
Polymer Structure Laboratory, Changchun Institute of Applied Chemistry, Academia Sinica, Republic of China

JEAN M. BRADY*, EDWIN L. THOMAS
Polymer Science and Engineering Department, University of Massachusetts, Amherst, Massachusetts 01003, USA

The microstructures of highly oriented drawn films of blends of high-density polyethylene (HDPE) and low-density polyethylene (LDPE) were investigated by transmission electron microscopy, electron diffraction, X-ray diffraction, and differential scanning calorimetry (DSC). The average crystal size, as well as long period, crystalline content, and melting endotherm peak, decreased as LDPE was added to the blend. When the LDPE content exceeded ~50%, the film texture changed from a single crystal texture to fibre symmetric. Segregation of the two polyethylenes was not detected at low LDPE contents in as-drawn or melted and recrystallized films. In the as-drawn films, a low temperature tail began to appear on endotherm melting peaks at LDPE contents ⩾70%, indicating the onset of segregation. In melt-crystallized films, however, two distinct melting endotherm peaks were visible for LDPE contents ⩾50%. An equilibrium melting point of 141° C and end surface free energy of 101 erg cm^{-2} (101 × 10^{-7} J cm^{-2}) were determined by use of the Thomson equation. The close agreement between these values and literature values for HDPE suggested that the crystals present in HDPE/LDPE blends were thermodynamically equivalent to HDPE crystals of equal size, implying that branches were excluded from the crystalline phase.

1. Introduction

In recent years, much of the emphasis of producing new polymeric materials has shifted to the practice of blending existing polymers. A basic tenet of blend technology rests on the fact that the properties of one homopolymer may be modulated by the addition of another. Quite often the resultant physical properties lie between the two extremes set by the homopolymers. In some cases, synergistic effects come into play. The way in which the homopolymers are blended and the state of mixing significantly affect the resultant properties. The separation of blends into distinct phases, as well as the size, connectivity, and time-development of each phase is important to the resultant physical characteristics.

In the present study, single-phase blends were fabricated by processing the material far from equilibrium. Specifically, highly oriented thin films were produced by crystallization in the presence of a high strain field [1]. The state of the material just prior to drawing is believed to be that of a gel containing small crystalline cross-links. Gel drawing of polyolefins has been studied elsewhere [2–4], and recently by us for HDPE [5, 6]. Using this processing technique [5–8], it has been possible to obtain solid solutions [8] or fine dispersions of crystals [9] for compatible melt blend systems of incompatible semicrystalline polymers.

2. Experimental details

The HDPE and LDPE samples employed were Marlex 6003 of Phillips (M_w = 200 000, M_w/M_n = 7 to 13) and LD-122 of Exxon (M_w = 286 000, M_w/M_n = 16), respectively. Chemically, the two polymers differ in branching characteristics. HDPE contains a negligible amount of short branches whereas LDPE contains a multitude of long and short branches. Highly oriented films of the blends of HDPE and LDPE were prepared according to the technique of Petermann and Gohil [7]. Polymer solutions of various HDPE/LDPE compositions were prepared at a concentration of 0.5% (wt/wt) in *o*-xylene. The film preparation temperature varied between 105 and 115° C depending on blend composition, higher LDPE compositions being produced at lower temperatures. For the individual homopolymers, the temperature chosen was usually a few degrees below the melting range of the solid polymer.

According to this preparation technique, hot polymer solution was spread uniformly on a preheated glass slide. The solvent was allowed to evaporate to the point where crystallization commenced. The resultant film was then sufficiently cohesive to be drawn vertically from the glass surface. The drawing rate was approximately 4 cm sec^{-1}. The application of strain, thermal quenching, and loss of solvent, inhibit significant segregation of LDPE and HDPE during the

* *Present address*: Mobil Chemical R and D, PO Box 240, Edison, New Jersey 08818-0240, USA.

0022–2461/88 $03.00 + .12

drawing process. Stresses are transferred through the film by means of existing crystals and entanglements. These elements pose constraints to chain mobility during subsequent recrystallization and segregation processes.

The as-drawn films were approximately 50 to 100 nm thick, and could thus be viewed directly by transmission electron microscopy. Thicker samples were made by stacking films together. These were used for X-ray diffraction and thermal analysis. Microscopy was carried out using a Jeol 100CX microscope operated at 100 kV. Samples were stabilized against dimensional changes by evaporating a thin layer of carbon on to the film surface.

The thermal behaviour of the samples was monitored with a Perkin-Elmer DSC-II differential scanning calorimeter (DSC). The heating and cooling rates used were 20° C min^{-1}.

Wide angle X-ray scattering (WAXS) profiles of the (1 1 0) and (0 0 2) reflections were recorded using a Siemens D500 wide-angle diffractometer in the reflection mode with nickel-filtered Cu$K\alpha$ radiation. The Rachinger correction [10] was applied to remove the Cu$K\alpha$-II peak contribution. The correction of the observed integral breadths for instrumental broadening was assumed to be of the form:

$$\Delta\beta_{obs} = \Delta\beta_L + \Delta\beta_i \quad (1)$$

where $\Delta\beta_{obs}$ indicates the measured integral breadth, $\Delta\beta_L$ is the broadening due to crystal size, imperfections, residual strains, and paracrystallinity, and $\Delta\beta_i$ is the instrumental broadening. It was assumed that $\Delta\beta_L$ was mainly a result of finite crystal size. The Scherrer equation was used to calculate the mean size L_{hkl} of the crystals (weight average)

$$L_{hkl} = K\lambda/(\Delta\beta_{L,hkl} \cos\theta_{hkl}) \quad (2)$$

K was taken to be 1.0 for the (1 1 0) and (0 0 2) reflections [11].

3. Results and discussion

Phase and diffraction contrast electron microscopy and electron diffraction were used to investigate the detailed morphologies of films of varying composition. Figs 1a to e show bright-field electron micrographs of these blends. In underfocused phase-contrast electron micrographs, the bright lines represent the lower density amorphous regions, while the grey areas between the bright lines are the high-density crystalline lamellar regions. Diffraction contrast results in the very dark regions which are crystals in the Bragg condition. It can be clearly seen that the lamellae consist of laterally aligned crystal blocks which are highly oriented along the draw direction. Corresponding electron diffraction patterns (see insets) corroborate a high degree of crystalline phase orientation, the chain axis being well aligned with the draw direction. WAXS line-broadening measurements indicate crystal widths (normal to c) are of the same order of magnitude as their thicknesses (parallel to c); verifying the block substructure of lamellae. The crystal thicknesses measured by (0 0 2) line broadening agree very well with values measured by bright-field electron microscopy.

Electron micrographs were used to quantify the number-average crystal size [12–15]. These films are particularly suitable for this due to the idealized structure of stacked lamellae. Numerical data from electron micrographs were obtained by measuring lamellar thicknesses and the corresponding long periods (Table I and Fig. 2). For pure HDPE, the average crystal thickness and long period were 24 and 32 nm, respectively. Crystal size, long period, enthalpic crystallinity, and melting temperature decreased as LDPE content increased (Table I). However, the linear crystallinity obtained from the ratio of the lamellar thickness to the long period (as measured by microscopy) was essentially invariant to LDPE content. This is likely due to the fact that lamellae become more segmented as branch content increases [16, 17]. Likewise the noncrystalline interface between adjacent crystalline blocks increases in size. Consequently, a one-dimensional estimate of crystallinity is not applicable because the crystalline phase cannot be assumed to be of infinite size in the lateral direction.

The reduction of the above quantities with addition of LDPE is due to the effect of branch point defects on crystallization. Branch points decrease chain symmetry and are excluded from the crystal lattice under equilibrium conditions [18, 19]. This exclusion results in a reduction of the equilibrium crystal thickness [20]. The reduction of melting temperature with LDPE content was related to the associated reduction of lamellar thickness (L) using the Thomson equation [21, 22]

$$T_m(L) = T_m^0(1 - 2\sigma_e/(\Delta hL) - 4\sigma_s/(\Delta hW)) \quad (3)$$

where T_m^0 is the equilibrium melting point of an infinitely large crystal, Δh is the heat of fusion per unit volume crystalline material, L is the crystal thickness (parallel to c), and σ_e is the end (fold) surface energy while σ_s is the side surface energy of the crystalline block. The crystal block width and depth were both assumed to equal W. This equation thus gives the

TABLE I Microstructural features of as-drawn HDPE/LDPE blends

Sample composition (% LDPE)	T_m (peak) (° C)	% Crystallinity (Enthalpic)	Lamellar thickness (nm)		Long period (nm)	Crystal width (nm)
			TEM (BF)	WAXS (0 0 2)	TEM (BF)	WAXS (1 1 0)
0	134	62	24	22	32	21
30	130	53	22	22	28	19
50	129	34	18	18	24	18
70	127	25	16	17	22	17
0	111	19	12	14	16	17

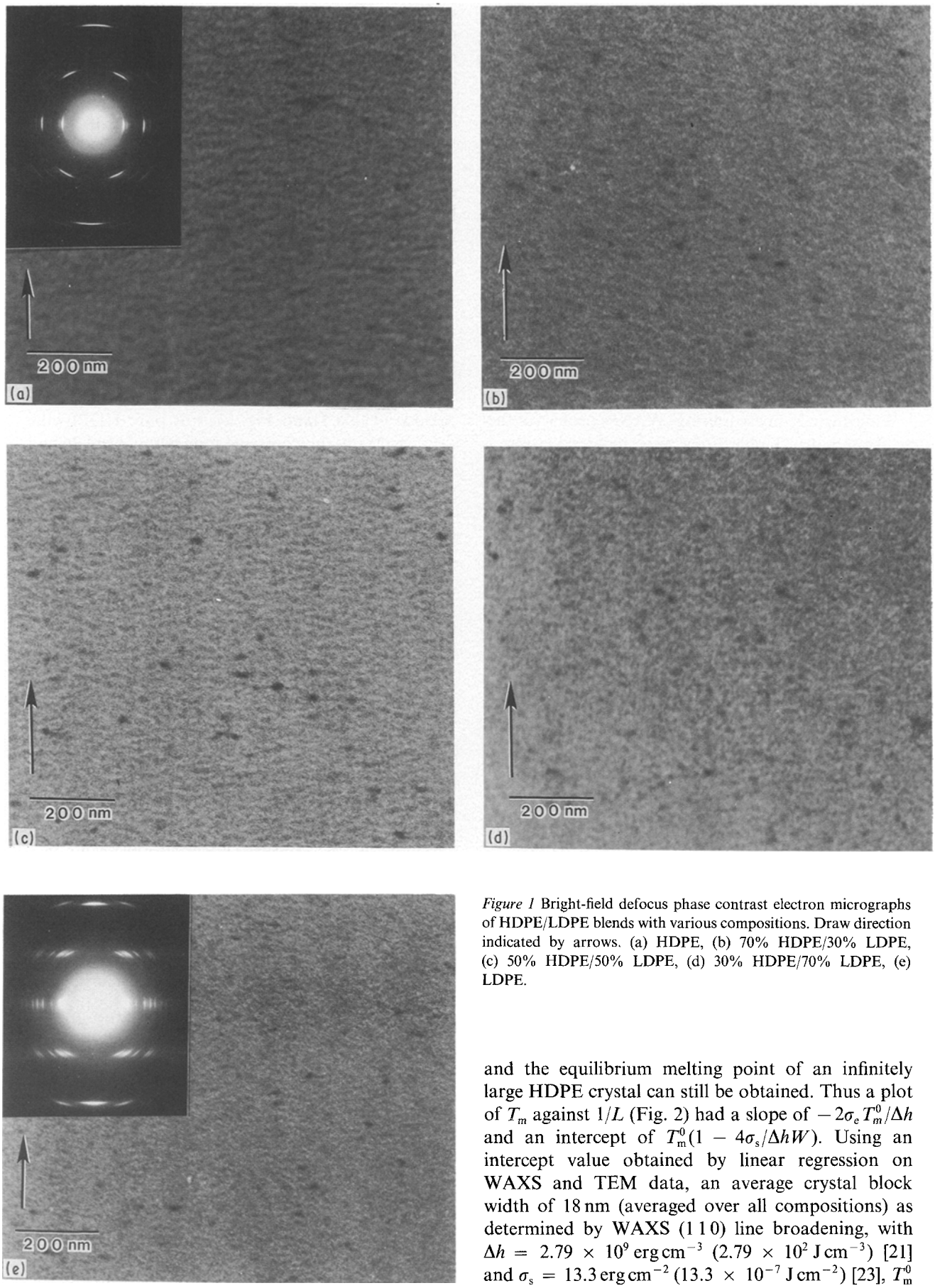

Figure 1 Bright-field defocus phase contrast electron micrographs of HDPE/LDPE blends with various compositions. Draw direction indicated by arrows. (a) HDPE, (b) 70% HDPE/30% LDPE, (c) 50% HDPE/50% LDPE, (d) 30% HDPE/70% LDPE, (e) LDPE.

melting point as a function of surface energy and crystal size. In the present case, the effect of branching on Δh, σ_e, and σ_s was neglected. In addition, although this equation is strictly applicable only to systems at equilibrium, an estimate of the end surface energy and the equilibrium melting point of an infinitely large HDPE crystal can still be obtained. Thus a plot of T_m against $1/L$ (Fig. 2) had a slope of $-2\sigma_e T_m^0/\Delta h$ and an intercept of $T_m^0(1 - 4\sigma_s/\Delta h W)$. Using an intercept value obtained by linear regression on WAXS and TEM data, an average crystal block width of 18 nm (averaged over all compositions) as determined by WAXS (1 1 0) line broadening, with $\Delta h = 2.79 \times 10^9$ erg cm^{-3} (2.79×10^2 J cm^{-3}) [21] and $\sigma_s = 13.3$ erg cm^{-2} (13.3×10^{-7} J cm^{-2}) [23], T_m^0 was calculated to be 141° C. This agreed well with the range reported by Wunderlich of 141 to 145° C for HDPE crystallized under equilibrium conditions. To obtain this value, however, it was necessary to omit data corresponding to pure LDPE, as these melting points were abnormally low for the crystal thicknesses measured by TEM and WAXS. This low thermal

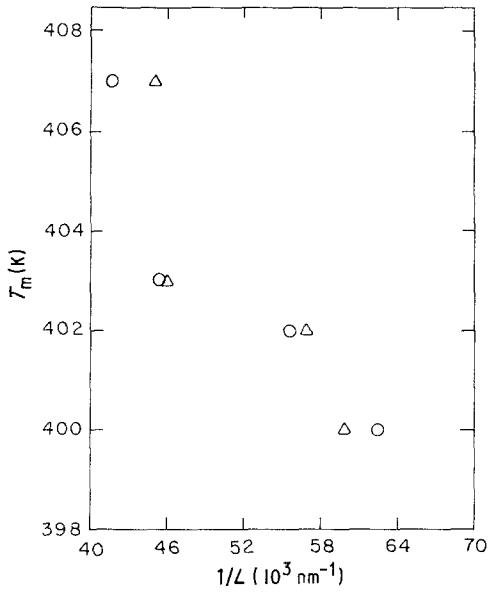

Figure 2 Melting point as a function of crystal thickness. (△) WAXS, (○) TEM.

stability of LDPE crystals suggests that branch points may have been incorporated into the crystal lattice to some extent, resulting in defective crystals. A slope of -3.0×10^{-5} yielded a fold surface free energy of $\sigma_e = 101\,\text{erg}\,\text{cm}^{-2}$ ($101 \times 10^{-7}\,\text{J}\,\text{cm}^{-2}$) (again, omitting the data for pure LDPE). This compared well with the literature value of $110\,\text{erg}\,\text{cm}^{-2}$ ($110 \times 10^{-7}\,\text{J}\,\text{cm}^{-2}$) [23].

The fact that each film was crystallized at different undercooling makes it difficult to determine the relative effects of branching with crystallization temperature on crystal size. One other variable which must be kept in mind is the degree of strain experienced by the film during processing. This too, would affect undercooling, because the extension of amorphous phase chains results in melting point elevation. This is due to the fact that the entropy of amorphous phase chains decreases upon extension, so that the entropy of fusion decreases [24].

The variation of diffraction intensity with rotation about the draw direction can be used to study film texture [6, 25]. In previous studies of HDPE, the intensity of the (1 1 0) reflection was maximized at a rotation angle of approximately 34° about the chain direction, while the (2 0 0) reflection was significantly increased and the (0 2 0) reflection significantly decreased [6]. This indicated the presence of a single crystal-like texture in these films; i.e. a texture in which the *b*-axis was preferentially oriented in the film plane. This same texture has been found in previous studies of HDPE [4]. A diffraction pattern of HDPE film, taken with the beam approximately parallel to the chain direction, shows explicitly this single crystal texture (Fig. 3), with the (1 1 0), (2 0 0), and (0 2 0) reflections forming arcs where the full width of half maximum angular breadth of the (0 2 0) reflection is $28 \pm 5°$.

Figs 4a to d show electron diffraction patterns as a function of rotation about the draw direction for various film compositions. (At a rotation angle of zero degrees, the electron beam is perpendicular to the film plane.) For LDPE contents at or lower than 30%, a single crystal texture was observed, indicating that low LDPE content had little effect on film texture. When the LDPE content exceeded ~50%, however, fibre symmetry about the chain axis was observed. This is similar to the fibre texture found in pure LDPE films prepared using the same gel-drawing process. Moreover, careful inspection of bright-field electron micrographs indicated a significant increase in the amount of diffracting crystalline phase as the LDPE content increased (Figs 1a to e). This can be interpreted in the following way. The dark, diffracting crystals imaged in bright-field are due predominantly to scattering from (1 1 0) crystal planes. For the single crystal-like texture, the (1 1 0) planes make an average angle of ~34° with the film surface normal. The number of (1 1 0) planes in the Bragg condition will be very small with the incident beam perpendicular to the film surface. For a symmetrical fibre texture, however, the (1 1 0) plane is randomly oriented about the chain axis. Thus, for any given film orientation with respect to the incident beam, the overall probability that some (1 1 0) planes are diffracting is much greater for the fibre symmetry case than for the single crystal-like texture case. As such, the diffraction contrast bright-field images corroborate the reciprocal space diffraction data.

It has been found that even with pure HDPE films,

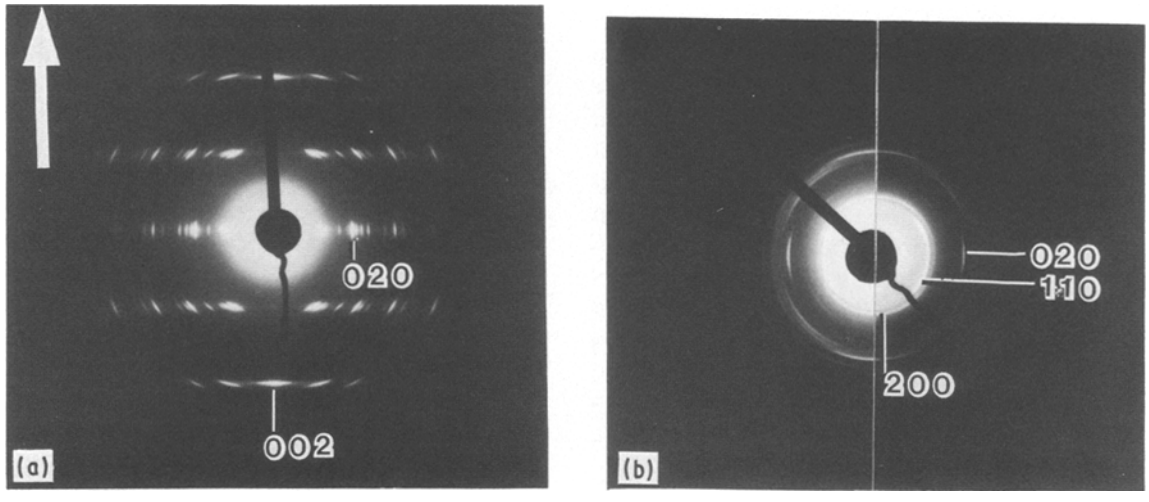

Figure 3 Electron diffraction patterns of HDPE taken with the electron beam (a) perpendicular to the film plane, (b) parallel to the chain axis. Note single crystal-like texture.

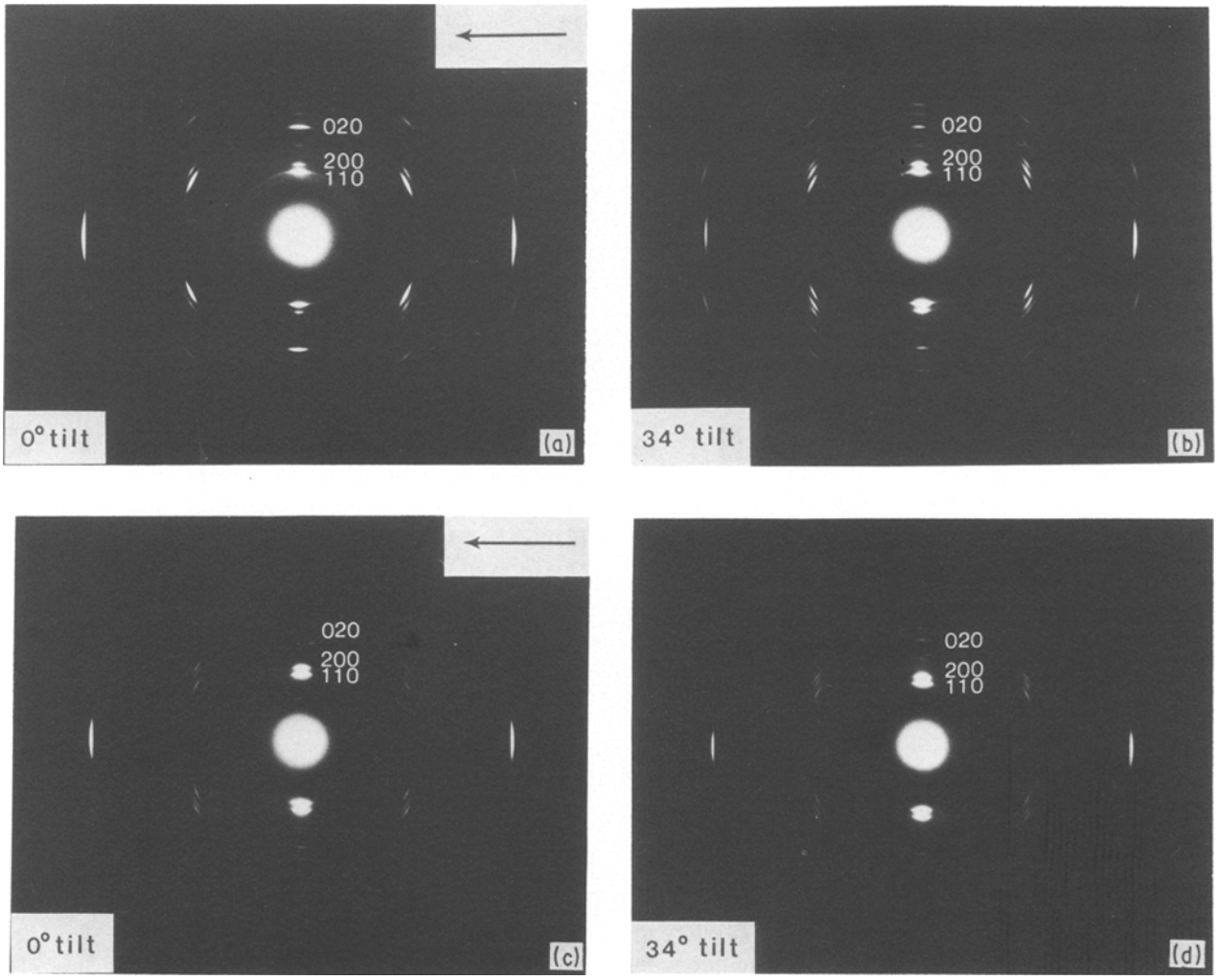

Figure 4 Electron diffraction patterns HDPE/LDPE blends as a function of composition and rotation angle about the draw direction. For (a) and (d) the beam was perpendicular to the draw direction. (a) 70% HDPE/30% LDPE, tilt angle = 0°, (b) 70% HDPE/30% LDPE, tilt angle = 34°, (c) LDPE, tilt angle = 0°, (d) LDPE, tilt angle = 34°.

two textures are possible: single crystal-like texture at low film preparation temperatures (up to 129° C) and fibre texture at higher temperatures (at or above 135° C). Fibre symmetry normally occurs for samples crystallized at low undercoolings. The presence of fibre symmetry at high LDPE contents implies that the effective undercooling of the film decreases as LDPE content increases, because the melting point of pure LDPE is less than that of pure HDPE.

To understand this phenomenon, it is necessary to explore those circumstances which give rise to the single crystal-like texture in the first place. Consider the crystallization of a very thin film. It is well known that for polyethylene, crystallization occurs fastest along the *b*-axis direction of the unit cell. Assume that a finite number of nuclei, with random orientation about the chain axis are present at the onset of crystallization and that the chain axis lies in the film plane. Once growth begins nuclei with their *b*-axis oriented in the film plane quickly grow until impingement, whereas nuclei with other orientations have their lateral growth restricted. Thus, crystallization kinetics dictate that the amount of crystalline material with the *b*-axis orientation in the film plane far exceeds that of any other axis orientation in the film plane, resulting in the single crystal-like texture.

As image contrast between different polyethylenes is essentially nonexistant for microscopy studies, DSC is very helpful in identifying phase separation. In the present case, all as-drawn films displayed a single endothermic peak (Fig. 5), indicating one crystal form was present. It was noted, however, that a low temperature tail was developing at high LDPE concentrations, corresponding to the presence of phase segregation. It should be emphasized that these films were never in the molten state. Instead, the dilute solution rapidly became concentrated, and was subsequently drawn. Therefore, the entanglement topology of these films is significantly different from that of melt-drawn films [2, 3].

Thermal analysis has indicated that segregation between branched and unbranched species does occur in polyethylene blend melts at sufficiently slow crystallization rates [26]. The as-drawn samples were melted in the DSC, held for 4 min at T_m + 10° C, then cooled at 20° C min^{-1} and the crystallization exotherms recorded (Fig. 6). Significant supercooling (overshoot of T_m) occurred due to the cooling rate used. Segregation between HDPE and LDPE was readily evident for LDPE contents exceeding 50%. This implies that in low LDPE content material, the LDPE was either excluded to the amorphous phase or co-crystallized

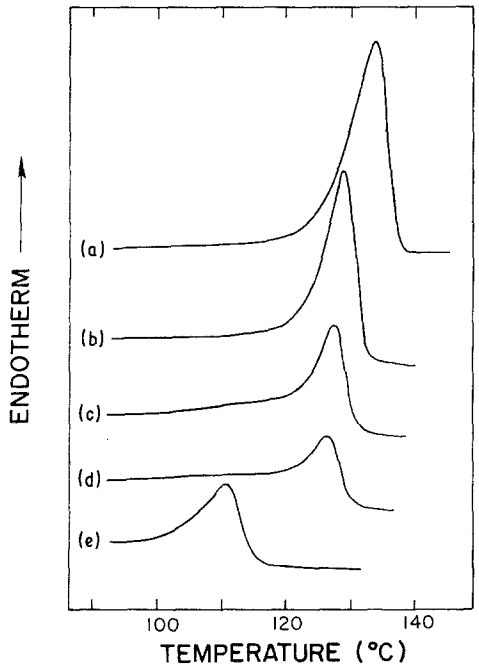

Figure 5 DSC endotherms of HDPE/LDPE as-drawn films with various compositions. Heating rate = 20° C min^{-1}. (a) HDPE, (b) 70% HDPE/30% LDPE, (c) 50% HDPE/50% LDPE, (d) 30% HDPE/70% LDPE, (e) LDPE.

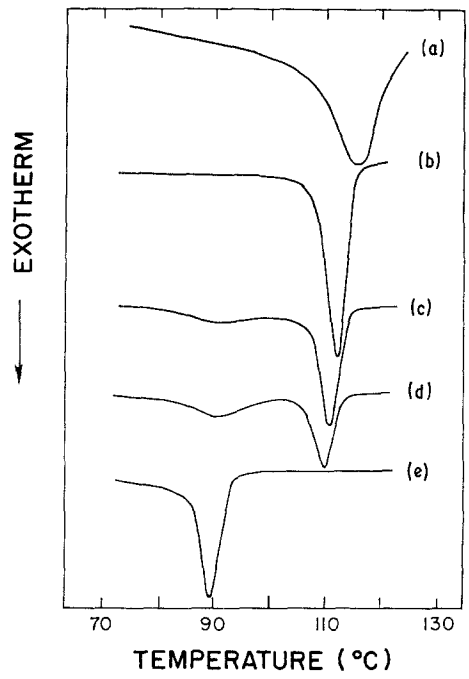

Figure 6 DSC exotherms of HDPE/LDPE melt blends with various compositions. Cooling rate = 20° C min^{-1}. (a) HDPE, (b) 70% HDPE/30% LDPE, (c) 50% HDPE/50% LDPE, (d) 30% HDPE/70% LDPE, (e) LDPE.

with HDPE. In fact, during nonisothermal crystallization, HDPE would be expected to crystallize first because it has a higher melting point and would therefore experience a greater undercooling than LDPE. The resultant constraints imposed on LDPE chain motion by HDPE crystals would then severely limit LDPE crystallization. This is supported by the sudden increase in population of low melting point crystals once HDPE is no longer present. The fact that a large melting point depression was evident even in single peak DSC endotherms indicates the LDPE did participate in and disrupt crystallization, resulting in lower crystallinities and a decrease of crystal size and perfection.

4. Conclusions

In this study, polymer films were crystallized under the influence of high strain and thermal quenching. These processing conditions were sufficiently far from equilibrium to hinder segregation between branched and unbranched polyethylenes. For co-crystallization of polymers with low thermal conductivity, an efficient alternative to thermal quenching is to rapidly increase solution concentration, as was done here prior to the application of strain. In both cases, the system undergoes a sudden increase in chain/chain interaction.

Films of varying LDPE/HDPE content were successfully made by a surface-drawing technique. Both of the polymers used were of equivalent molecular weights. With increasing LDPE content in blends, crystal size, long period, crystallinity and melting temperatures all decreased with respect to those of pure HDPE. This can be understood in terms of the disruption of crystallization by branch points. The close correspondence between T_m^0 and σ_e values found for blends and literature values for HDPE suggested that the crystals in these blends were thermodynamically equivalent to HDPE crystals of the same size. This indicates that branches were, in fact, excluded from crystals in HDPE/LDPE blends. In pure LDPE, however, abnormally low melting points for a given crystal size suggested that some branches were incorporated into crystals, constituting defects. Thermal analysis of melt crystallized blends indicated that segregation only occurred at LDPE contents exceeding 50%. For lower LDPE contents, the two stage crystallization process was supressed by the rapid and extensive solidification of the HDPE component.

Acknowledgements

The financial support of the National Science Foundation, grant no. DMR 84-06079 (Polymers Division) is gratefully acknowledged. The authors also thank Mr X. Jin for DSC measurements.

References

1. I. L. HAY, M. JAFFE and K. F. WISSBRUN, *J. Macromol. Sci. Phys Edn.* **B12** (1976) 423.
2. P. SMITH and P. J. LEMSTRA *Colloid Polym. Sci.* **258** (1980) 891.
3. P. SMITH, P. J. LEMSTRA and H. C. BOOIJ, *J. Polym. Sci. Phys. Edn.* **19** (1981) 877.
4. P. SMITH, P. J. LEMSTRA, J. P. L. PIJPERS and A. M. KIEL, *Colloid Polym. Sci.* **259** (1981) 1070.
5. J. M. BRADY and E. L. THOMAS, to be published.
6. D. C. YANG and E. L. THOMAS, *J. Mater Sci.* **19** (1984) 2098.
7. J. PETERMANN and R. M. GOHIL, *ibid.* **14** (1979) 2260.
8. R. M. GOHIL and J. PETERMANN, *J. Macromol. Sci. Phys Edn.* **B18** (1980) 217.
9. J. PETERMANN and R. M. GOHIL, *J. Polym. Sci. Polym. Lett. Edn.* **18** (1980) 781.
10. W. A. RACHINGER, *J. Sci. Instrum.* **25** (1948) 254.
11. A. R. STOKES and A. J. C. WILSON, *Proc. Camb. Phil. Soc.* **40** (1944) 197.
12. I. G. VOIGHT-MARTIN, *J. Polym. Sci. Phys. Edn.* **18** (1980) 1513.

13. G. R. STROBL, M. J. SCHNEIDER and I. G. VOIGHT-MARTIN, *ibid.* **18** (1980) 1361.
14. I. G. VOIGHT-MARTIN, L. MANDELKERN and E. W. FISCHER, *ibid* **18** (1980) 2347.
15. *Idem, ibid.* **19** (1981) 1769.
16. L. MANDELKERN, *Polymer J.* **17** (1985) 337.
17. I. G. VOIGHT-MARTIN, R. ALAMO and L. MANDELKERN, *J. Polym. Sci. Phys. Edn.* **24** (1986) 1283.
18. R. ALAMO, R. C. DOMSZY and L. MANDELKERN, *J. Phys. Chem.* **88** (1984) 6587.
19. J. VILE, J. HENDRA, H. A. WILLIS, M. E. A. CUDBY and A. BUNN, *Polymer* **25** (1984) 1173.
20. P. J. FLORY, *J. Chem. Phys.* **17** (1949) 223.
21. B. WUNDERLICH, in "Macromolecular Physics", Vol. 3, Crystal Melting (Academic, New York, 1973) p. 30.
22. W. THOMSON, *Phil. Mag.* **42** (1871) 448.
23. F. P. PRICE, *J. Chem. Phys.* **35** (1961) 1884.
24. H. G. ZACHMANN, in "Statistical Mechanics, Foundations and Applications", Proceedings of IUPAC Meeting, Copenhagen 1966, edited by T. A. Bak (Benjamin, New York, 1967) p. 237.
25. J. PETERMANN and J. GLEITER, *Phil. Mag.* **28** (1973) 1279.
26. D. R. NORTON and A. KELLER, *J. Mater. Sci.* **19** (1984) 447.

Received 21 July
and accepted 23 October 1987